Paper No. 770. (quote when citing this article)
Eleventh World Conference on Earthquake Engineering
ISBN: 0 08 042822 3

IDENTIFICATION OF STRUCTURAL SYSTEMS FROM MICROTREMORS AND ACCURACY FACTORS

YUKIO NAITO and TOSIHISA ISHIBASHI
Kajima Technical Research Institute,Kajima Corporation
19-1,Tobitakyu 2-chome,Choufu-shi,Tokyo,182,Japan

ABSTRACT

Microtremors of an 18-story reinforced-concrete building were measured under various wind velocities for about one year. They were analysed and a simulation study was conducted for better system identification of buildings subject to small vibrations caused by ground motions (microtremors) and wind force. In particular, the effect of wind force on system identification was studied using these data. The phenomenon of wind velocity affecting the damping ratio obtained from the transfer function was also studied using observation data and analysis. The transfer functions, power spectra, natural frequencies and damping ratios from the measurement, simulation model and other simple models were compared.

KEYWORDS

Microtremors; Measurement; System Identification; Wind Force; Wind Velocity; Ground Motion; Damping Ratio; Natural Frequency; Transfer Function; Power Spectrum

INTRODUCTION

Advantages of microtremor measurement for system identification of structures include the lack of a need for exciters, the possibility of statistically processing great quantities of data, and the possibility of learning about structural vibrations caused by ground motions. Disadvantages include the relatively large effect of noise because of the small signal amplitudes and the complexity of input mechanisms of combined ground motions and wind forces. The last factor makes it especially important to study accuracy and limitations of microtremor measurement for system identification.

The authors measured microtremors of an 18-story reinforced-concrete (RC) building with an anemometer at the top of it under various wind velocity conditions for about one year. They studied system identification of buildings subject to small vibrations caused by ground motions (microtremors) and especially by wind forces, using these data (Ishibashi and Naito, 1994). The results showed the following : 1) the natural frequency obtained from microtremor measurement is only slightly affected by wind velocity ; 2) wind velocity has little effect on the damping ratio obtained from the power spectrum of the top of a building, but larger wind velocity makes the damping ratio obtained from the transfer function larger ; and 3) a model of particles with a sway-rocking spring at the base makes a good simulation.

This paper presents results of the measurement and simulation discussed above and studies the phenomenon

where wind velocity affects the damping ratio obtained from the transfer function. Transfer functions are required to determine phase lags between measuring points and vibration modes. There are presumed to be three main causes of variations in obtained damping ratios. This paper examines these three factors using simple models, and shows the contributions of these three factors to the phenomenon.

WIND AND MICROTREMOR MEASUREMENT

Object and Method of Measurement

The object of measurement was the 18-story RC-apartment building shown in Fig. 1. Microtremors were measured for about one hour in each of the nine cases listed in Table 1. Locations of displacement sensors and the anemometer are also shown in Fig. 1. This paper discusses responses in the short side (NS) direction and vibrations of ground (base) and roof. Human powered free vibration at the first frequency at the roof was also measured.

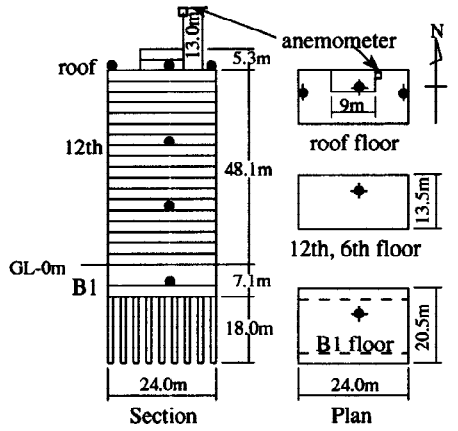

Fig.1. Outline of the building(● : sensor)

Table 1. Case for measurement

Case	wind		rms of roof response
	direction	av. vel.	
1	N	1.5 m / sec	4.2 μ m
2	NE	3.6 m / sec	4.1 μ m
3	E	3.9 m / sec	3.9 μ m
4	S	4.2 m / sec	4.0 μ m
5	W	4.3 m / sec	4.9 μ m
6	NE	6.7 m / sec	5.0 μ m
7	N	10.7 m / sec	15.7 μ m
8	N	12.5 m / sec	18.8 μ m
9	S	13.2 m / sec	25.4 μ m

Method of Data Analysis

Transfer functions ((cross-spectrum of I/O) / (power spectrum of I)), power spectra and the coherencies of measuring points (with respect to the base) were calculated from time series records. Thirty-six frames, each of which consists of 100 second data acquired at a sampling frequency of 40.96Hz, were used for averaging. Figure 2 shows ratios of damping ratios for the first frequency obtained from power spectra to 1.8% from free vibration versus number of times for averaging. The damping ratio obtained from free vibration is used instead of the real damping ratio because the real value is unable to be known. Above 36 frames, the ratio converges to a value slightly smaller than the value for free vibration. This value is considered to be appropriate if the difference in amplitude (about 400 μ m for free vibration and 3.9 μ m to 5.0 μ m for microtremors) is taken into consideration.

Results and Discussion

Frequency and Mode for Each Eigenvalue. Figure 3 shows a transfer function of the roof to the base and vibration modes (first : 1.0Hz, second : 3.3Hz, third : 5.8Hz) for Case 3, where wind velocity is small. According to the amplitude for each mode, the effect of wind force is clear at the first frequency. The resulting first mode vibration is discussed below.

Transfer Function, Power Spectrum and Coherency. Figure 4 shows transfer functions of the roof to the base, coherencies and power spectra at frequencies around the first peak for two typical cases. The statements below can be made.

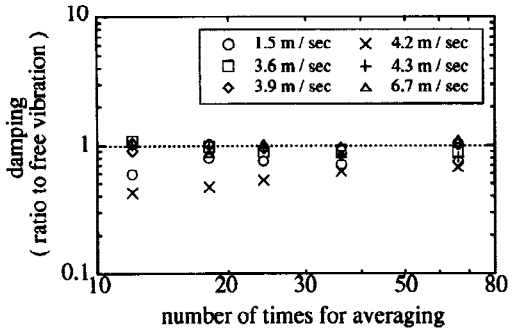

Fig.2. Obtained damping vs. averaging number

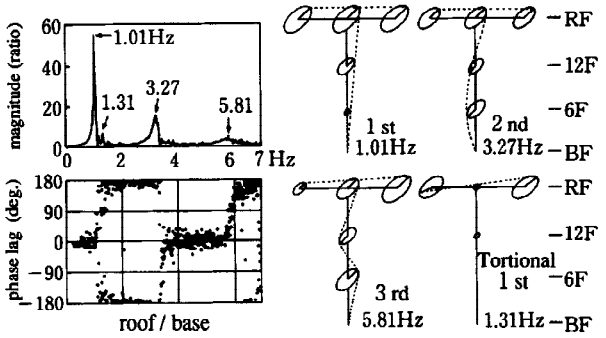

Fig.3. Transfer function and mode

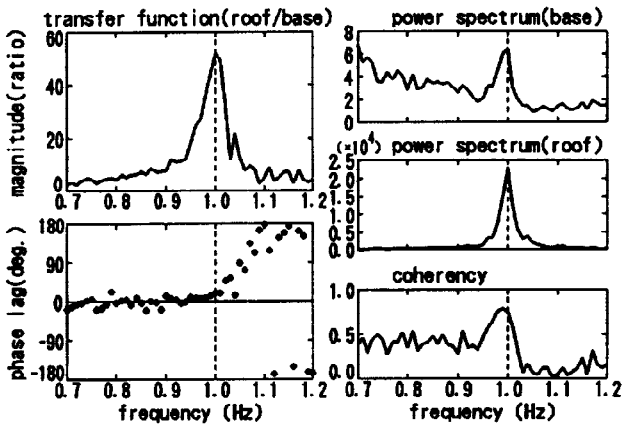

(a) Case 1 1.5m/sec

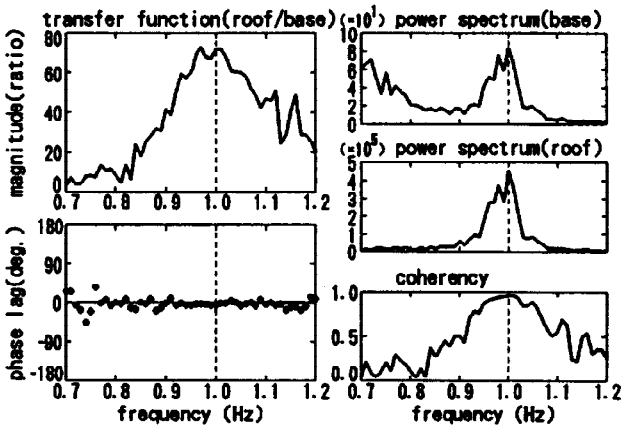

(b) Case 9 13.2m/sec

Fig.4. Observation trasfer function, power spectrum and coherency
- unit for power spectrum (μ m · sec)^2 -

a) The peak of the transfer function becomes wider and the damping ratio obtained by the half power method becomes larger as wind velocity becomes larger. The magnitude of the peak of the transfer function also becomes larger as wind velocity becomes larger.
b) The phase lag of the transfer function is small up to the first frequency peak even when wind velocity is small. This is different from the phase lag of transfer functions for systems with fixed base and ground motion.
c) The amplitude of the power spectrum for the base around the first peak as well as for the roof becomes larger as wind velocity becomes larger.

First Frequency and Damping Ratio . Table 2 shows the first peak frequencies and damping ratios obtained by the half power method for all cases, derived from transfer functions and power spectra. Figure 5 shows damping

Table 2. Observation first frequency and damping ratio from transfer function and power spectrum

Case	wind		transfer function			power spectrum	
	direction	velocity	1st freq.	peak ratio	damping	1st freq.	damping
1	N	1.5 m/sec	1.00 Hz	53.6	1.6 %	1.00 Hz	1.3 %
2	NE	3.6 m/sec	0.99 Hz	56.7	1.3 %	0.99 Hz	1.7 %
3	E	3.9 m/sec	1.01 Hz	55.9	1.9 %	1.00 Hz	1.7 %
4	S	4.2 m/sec	0.99 Hz	55.2	1.2 %	0.97 Hz	1.1 %
5	W	4.3 m/sec	0.99 Hz	64.1	1.8 %	0.99 Hz	1.5 %
6	NE	6.7 m/sec	0.97 Hz	53.1	2.4 %	0.97 Hz	1.5 %
7	N	10.7 m/sec	0.97 Hz	70.0	5.1 %	0.97 Hz	2.3 %
8	N	12.5 m/sec	0.95 Hz	78.6	5.6 %	0.95 Hz	2.5 %
9	S	13.2 m/sec	1.01 Hz	71.4	7.5 %	1.00 Hz	3.7 %

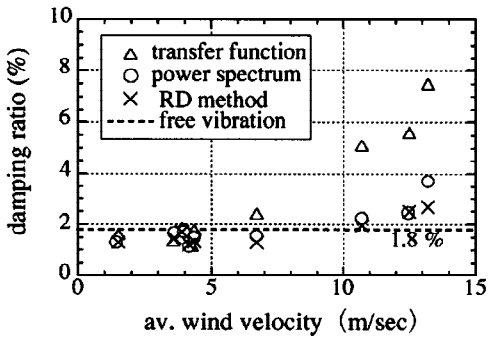

Fig.5. Damping ratio for the first peak vs. av.wind vel.

ratios obtained using the half power method from transfer functions and power spectra, as well as damping ratios obtained using the RD method (Tamura *et al.*, 1991), vs. average wind velocity.

a) Values of first peak frequencies obtained from transfer functions and power spectra are almost the same, ranging from 0.95 Hz to 1.01 Hz for the nine cases.
b) Wind force influences damping ratios obtained from the transfer functions. The damping ratios are about 1.8% under small wind velocity conditions, but are larger when wind velocity is above 10 m/sec.
c) Wind force has little influence on damping ratios obtained from power spectra. Power spectra in this case represent the response of a system with soil-structure interaction. Damping ratios from power spectra are very close to those obtained using the RD method. They increase slightly with wind velocity, and this is probably because of the dependency of damping ratio on amplitude.

SIMULATION

Model and Method for Analysis

Results of ground motion and wind force simulations are compared with observation data. The simulation model is for the short side (NS) direction of the building and consists of 19 particles, a base and a sway-rocking spring (see Fig. 1 and 6). Damping ratios of 1% and 10% (viscous damping) are assumed for the superstructure and the base, respectively.

Table 3 compares the natural frequencies for three modes and the damping ratio for the first peak with values calculated from observation data for Case 1. The damping ratio from free vibration is employed for the observation results. The two sets of values coincide well.

Artificial independent ground motion and wind force are used as input to the model, as shown in Fig. 6. Responses of the model were processed using the procedures used for observation data to obtain transfer functions, power spectra and coherencies.

The artificial ground motion is a random wave and has flat power below 10Hz. The standard deviation of the amplitude is 0.002 cm/sec^2 (Gal), which gives base amplitudes consistent with observation data.

Fluctuating wind velocities at the heights of particles were calculated using Iwatani's multi dimensional auto-regressive method (Iwatani, 1982), assuming average wind velocity at the height of the anemometer (about 60m) to be 5, 7, 10, or 15 m/sec and considering auto and cross-correlations between heights. The distributions of average and fluctuating wind velocities and the power spectra densities of fluctuating wind velocity for the target were decided according to Recommendations for Loads on Buildings of the AIJ (1993).

Table 3. Peak frequency and damping ratio from simulation and observation

mode	simulation		observation	
	freq.	damping	freq.	damping
1 st	1.02 Hz	1.4 %	1.00 Hz	1.8 %
2 nd	3.08 Hz	--------	3.21 Hz	--------
3 rd	5.14 Hz	--------	5.78 Hz	--------

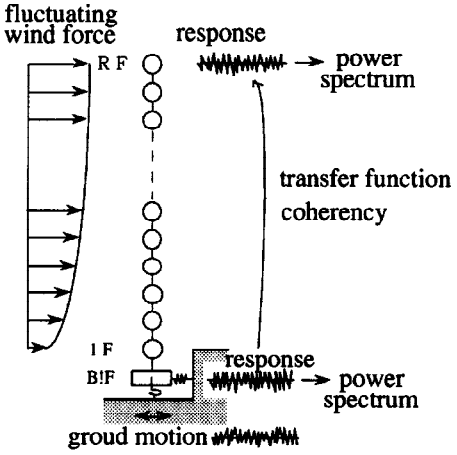

Fig.6. Outline of simulation

Results and Discussion

Transfer Function, Power Spectrum and Coherency. Figure 7 shows transfer functions, power spectra and coherencies around the first peak obtained from simulation results. Figure 7 can be compared with Fig. 4.

Simulation results agree well with observation results with respect to the shape and phase lag of the first peak and their dependency on wind velocity, the relations between power spectra of the base and the roof, and the shape of coherency.

First Frequency and Damping Ratio. Table 4 shows the first frequencies and damping ratios for all simulation cases, obtained from transfer functions and power spectra. The results agree well with the values shown in Table 2 with respect to the points identified below.

a) The first frequencies from transfer functions and power spectra are almost identical.
b) The magnitudes of transfer functions increase with wind velocity.
c) Damping ratios evaluated from transfer functions are overestimated under strong wind conditions, but those evaluated from power spectra hardly change with wind force.

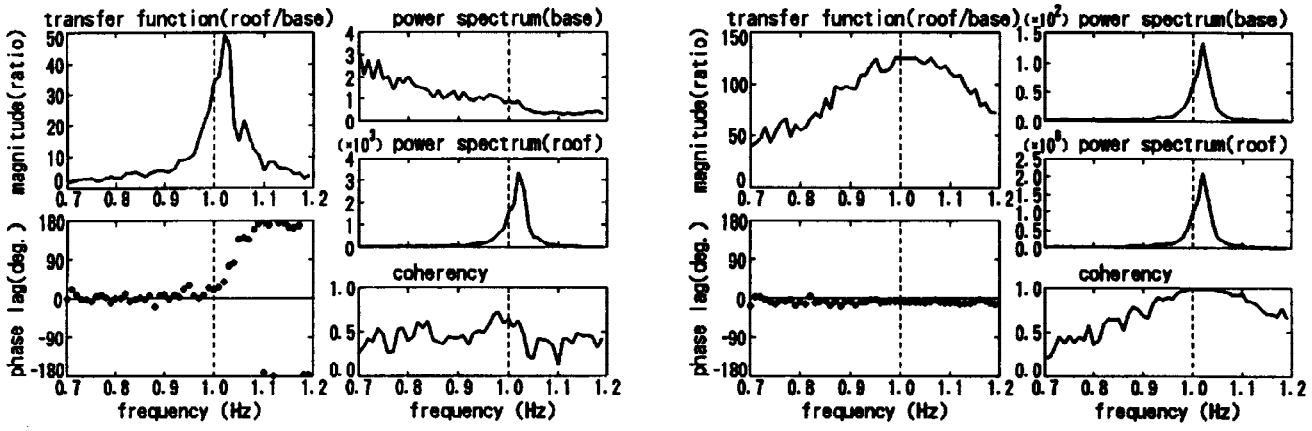

Fig.7. Simulation transfer function, power spectrum and coherency
- unit for power spectrum (μ m / sec)^2 / (2 π f)^4 -

Table 4. Firsts frequency and dumping ratio from transfer function and power spectrum for simulation

Case	ground motion	wind force	transfer function			power spectrum	
	S.D.	av. vel.	1st peak	peak ratio	damping	1st peak	damping
a	0.002 Gal	--------	1.03 Hz	49.3	1.4 %	1.02 Hz	1.3 %
b	0.002 Gal	5 m/sec	1.02 Hz	49.9	1.4 %	1.02 Hz	1.5 %
c	0.002 Gal	7 m/sec	1.02 Hz	82.7	1.8 %	1.02 Hz	1.6 %
d	0.002 Gal	10 m/sec	1.03 Hz	116.3	4.2 %	1.02 Hz	1.6 %
e	0.002 Gal	15 m/sec	1.04 Hz	124.6	13.3 %	1.02 Hz	1.7 %

MECHANISM OF DEFORMATION OF TRANSFER FUNCTION

The three main causes of transfer function deformation are presumed to be as follows : 1) a system with soil - structure interaction receives (wind) force at its upper part ; 2) two types of input force (wind force and ground motion) exist ; 3) the two input forces are independent. Here, these three factors are studied using simple models, and contributions of these three to the deformation of the transfer function are shown.

System with Input Force at its Upper Part

Multiparticle System with Wind Force Alone. A system which receives only wind force is studied here as an example of a case in which wind force is very strong and the effect of ground motion is practically negligible. The model and the wind force are the same as those of the simulation described above. A wind force of 15 m/sec was applied to the model and the results shown in Fig. 8 were obtained. Considering the good coincidence with observation of the simulation with this model, wind force and ground motion, the result shown in Fig. 8 can be regarded as a simulation for cases in which wind force is much stronger than inertial force. The following can be concluded.

a) The shape of the transfer function around 1.03 Hz, which is the first peak of the super -structure (19 particles) under fixed base condition, is similar to those for strong wind shown in Fig. 4 (b) and Fig. 7 (b).
b) The magnitude has hollows around 2, 4, 6 and 8 Hz, and the phase shows sudden changes there.

System with Sinusoidal Input Force at the Top. A multiparticle model with sinusoidal force applied at the top was studied as an extreme example of a system with input at its upper part. A "19 particle system" consisting of 19 particles and a base was studied (see Table 5). For simplicity, only horizontal movement is taken into consideration. The weights of the particles and the base are nearly equal to those of the simulation model. The sway spring was obtained by equivalent conversion from the sway-rocking spring of the simulation model. The superstructure spring constants and damping coefficient were evaluated so that the first frequency is 1Hz and the damping ratio for 1Hz is 1% in the fixed base condition.

9.8×10^3 N (1 tonf) force acts on the top of the 19-particle model discussed above. Figure 9 shows the response of the top and Fig. 10 shows the transfer function. The phase of the response is the phase lag from the acting force. The following can be concluded.

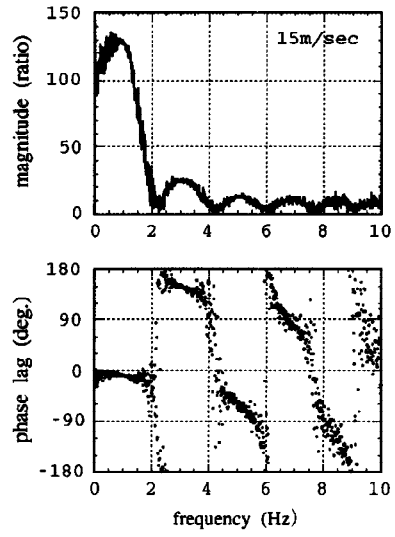

Fig.8. Transfer function for wind force alone condition

Table 5. Outline of 19 and 1 particle model

	model	19 particle	1 particle
superstructure	particle mass (ton)	300	4735
	spring (ton / cm)	1862	191
	damping coefficient (sec)	0.003183	0.003183
base	mass (ton)	8000	8000
	sway spring (ton / cm)	2905	2905
	damping coefficient (sec)	0.03183	0.03183
1st peak	frequency (Hz)	0.965	0.965
	damping ratio (%)	1.62	1.60

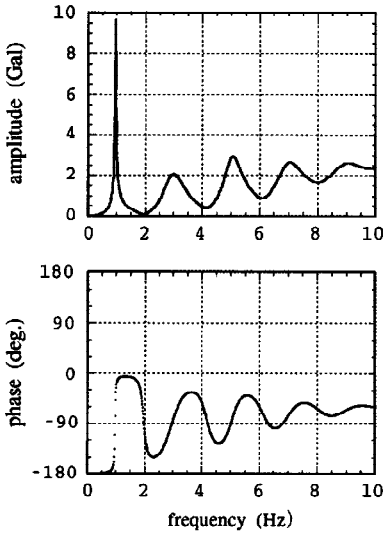

Fig.9. Response of the top

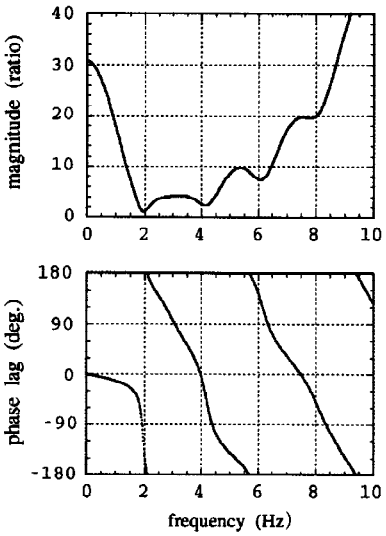

Fig.10. Transfer function for Top / Base

a) The response of the top and the transfer function are different.
b) The transfer function of the 19-particle model is similar to that shown in Fig. 8 for the wind-force-only condition, although there is some difference in magnitude around 1Hz which is the first peak in the fixed base condition.

Summary of Transfer Functions of Systems on the Upper Part on which Force Acts. As stated above, the following can be concluded concerning transfer functions of the 19 particle model with wind force alone and with sinusoidal force at the top.

a) Results from the 19-particle simulation model with wind force only are similar to observation transfer functions under strong wind conditions.
b) The 19-particle model with sinusoidal force on the top gives similar results.
c) Accordingly, a major cause of the widening of the transfer function peak and the damping ratio increase obtained using the half power method for strong wind conditions is the mechanism and system itself whereby force acts on the upper part of a structure.
d) There is some difference in magnitude around 1Hz. Therefore, there is some possibility of other causes.

System with Sinusoidal Ground Motion and Force on the Upper Part

Two dependent input forces, i.e. with a phase lag between them, act on a system. The transfer function, especially the widening of the peak, is studied. For simplicity, the 1-particle model described in Table 5 is used. Ground motion is 1 cm/sec^2 (Gal). Force on the top is from $5 \times 9.8 \times 10^3$ N (5 tonf) to $50 \times 9.8 \times 10^3$ N (50 tonf). Phase lag between the two input forces is varied as a parameter.

Transfer functions for all phase lags (varying by 5 degrees) were averaged as complex numbers. This corresponds approximately to averaging data frames in which each frame has a different phase lag between two inputs. Figure 11 shows the results. The following can be stated.

a) Averaging makes transfer functions widen, similar to that shown in Fig. 4. Larger force on the upper part makes peaks of the transfer functions wider.
b) A 1-particle model with a base, sway spring and two dependent input forces gives results more similar to those from the observation data than with the factor in Fig. 8 ~ Fig. 10 above alone. Therefore, the situation of ground motion and force on the upper part is concluded to also be a major cause of the phenomenon.

Transfer Function of a System with Independent Ground Motion and Force on the Top

Independent random ground motion and force on the top act on the 1-particle model described previously. The random wave has uniform power in the range from 0 Hz to 20 Hz, and its amplitude is evaluated by rms. Ground motion is 1 cm/sec^2 (Gal), and force on the top is $5 \times 9.8 \times 10^3$ N (5 tonf) or $20 \times 9.8 \times 10^3$ N (20 tonf). Figure 12 shows the results, which can be compared with those from observation data (Fig. 4) and those of simulation by the 19-particle model with a sway rocking spring (Fig. 7). The following can be concluded.

a) The 1-particle model with two independent random inputs gives results more similar to those from observation and simulation data than the results in Fig. 8 ~ Fig. 11.
b) Accordingly, two independent random inputs are also a major cause of the widening of the transfer function peak under strong wind conditions.

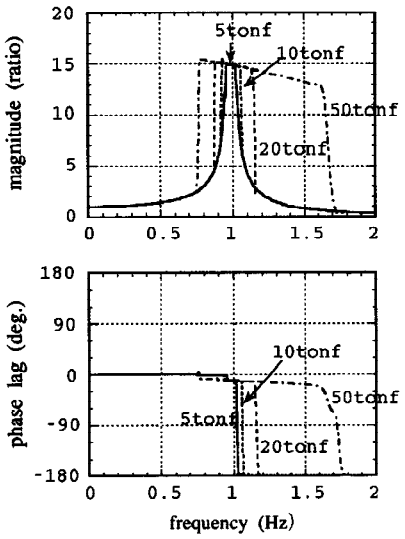

Fig.11. Average of 72 transfer functions (at intervals of 5 degrees)

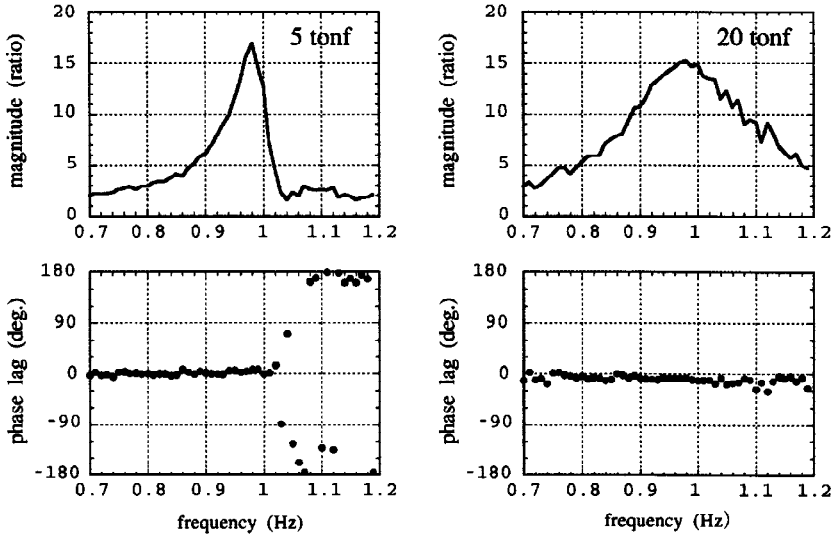

Fig.12. Transfer function for two independent randam imputs

CONCLUSION

System identification of buildings subject to small vibrations caused by ground motion (microtremors) and wind force was studied. The following conclusions were drawn : 1) natural frequency obtained from microtremor measurement is hardly affected by wind velocity; 2) wind velocities have little effect on damping ratios obtained from power spectra of the top of a building, but wind velocities make damping ratios obtained from transfer functions larger ; 3) a multiparticle model with a sway-rocking spring at the base makes a good simulation.

The phenomenon of wind velocity affecting damping ratios obtained from transfer functions was studied using observation data and analysis. The main cases of variation in obtained damping ratios are : 1) when a system with soil-structure interaction receives (wind) force at its upper part ; 2) when there are two types of input force (wind force and ground motion) ; 3) when there are two independent input forces.

REFERENCES

Architectural Institute of Japan (1993). *Recommendations for loads on buildings* (in Japanese).

Ishibashi, T. and Y. Naito (1994). Influence of wind force on system identification of tall buildings during microtremors. *Journal of structural and construction engineering* (Transactions of A.I.J.) , 464, 71-80 (in Japanese with English abstract).

Iwatani, Y. (1982). Simulation of multidimensional wind fluctuations having any arbitrary power spectra and cross spectra , *Journal of Wind engineering* , 11 , 5-18 (in Japanese with English abstract).

Tamura, Y., A. Sasaki and H. Tsukagoshi (1991). Evaluation of damping ratio of randomly excited structures. *Journal of Wind engineering* , 47, 93-94 (in Japanese).